Functionalized Pyrazoles as Agents in C–C Cross-Coupling Reactions

Marijana Pejic, Sebastian Popp, Michael Bolte, Matthias Wagner, and Hans-Wolfram Lerner

Institut für Anorganische Chemie, Goethe-Universität Frankfurt am Main, Max-von-Laue-Straße 7, 60438 Frankfurt am Main, Germany

Reprint requests to Dr. Hans-Wolfram Lerner. Fax: ++49-69-79829260. E-mail: lerner@chemie.uni-frankfurt.de

Z. Naturforsch. **2014**, *69b*, 83 – 97 / DOI: 10.5560/ZNB.2014-3224
Received August 14, 2013

The 1-tetrahydropyranyl-(THP-)protected pyrazoles 4-R-pz(THP) (R = pinacolatoboryl = Bpin (**3a**(THP)), Me_3Si (**4a**(THP)), Me_3Sn (**5a**(THP)), and 4-R-3,5-Ph_2pz (R = Bpin (**3b**(THP)), Me_3Si (**4b**(THP)), Me_3Sn (**5b**(THP)) were obtained by the following syntheses: i) In a first step, 4-X-pz (X = Br (**1a**), I (**2a**)) and 4-X-3,5-Ph_2pz (X = Br (**1b**), I (**2b**)) were reacted with 3,4-dihydro-2*H*-pyran (DHP) to give the related THP-protected bromo- or iodopyrazole derivatives. ii) In a second step these THP derivatives were metalated by treatment with *n*BuLi or *i*PrMgCl. Subsequent reactions of the THP-protected metallopyrazoles 4-*M*-pz(THP) and 4-*M*-3,5-Ph_2pz(THP) (*M* = Li, MgBr) with Bpin(O*i*Pr), Me_3SiCl, and Me_3SnCl yielded the pyrazole derivatives **3a**(THP), **3b**(THP), **4a**(THP), **4b**(THP), **5a**(THP), and **5b**(THP). In contrast to the stannylated pyrazoles **5a**(THP) and **5b**(THP), the corresponding borylated and silylated derivatives could be easily deprotected: treatment of **3a**(THP), **3b**(THP), and **4a**(THP) with HCl yielded the parent pyrazoles **3a**, **3b** and **4a**. The microwave-assisted C–C cross-coupling reactions of these pyrazoles with aryl halides were examined, *e. g.* Suzuki reactions of **3a** with *p*-pentylphenylbromide, *p*-hexylphenylbromide, and *p*-(2-ethylhexyl)phenylbromide. Similar reactions were also performed with **1a**, **1b**, **2a**, and **2b** and aryl-substituted pinacolatoboranes or boronic acids. Crystals of **5b**(THP) suitable for X-ray diffraction were grown (monoclinic $P2_1/c$) and their structure determined. The crystal structures of **1a**·HBr (monoclinic $P2_1/n$), **1b** (triclinic $P\bar{1}$), (**1c**)$_2$·HBr (monoclinic $P2/c$), **1c**·HBr·$(Br_2)_{0.5}$ (triclinic $P\bar{1}$), (**2a**)$_3$·H_2SO_4 (triclinic $P\bar{1}$), **3a** (orthorhombic $P2_12_12_1$), (**3a**)$_3$·H_2O (trigonal $R3c$), **3b** (orthorhombic $Pna2_1$), and **4a** (monoclinic Pc) reveal interesting hydrogen bonding networks.

Key words: Pyrazoles, C–C Cross-Coupling, Luminescence, X-Ray Structure Analysis, Hydrogen Bonding Networks

Introduction

Multidentate ligand systems have attracted considerable interest in the last decades. Prominent examples of this class of ligands are the (pyrazol-1-yl)borates (scorpionates) $[R_nBpz_{4-n}]^-$ (R = H, alkyl, aryl; $n = 2, 1, 0$; pz = pyrazol-1-yl) [1 – 8]. Scorpionates have found applications in a wide range of chemistry, from modelling the active site of metalloenzymes, through analytical chemistry and organic synthesis to catalysis and materials science [9].

However, degradation reactions of these scorpionate ligands were often observed in the presence of transition metal salts MX_n, [10 – 12]. We found that deboronation of scorpionates easily takes place if the metal center in MX_n is more Lewis acidic than the boron center in the corresponding borane of the pyrazolyl borate (Fig. 1). In these cases there is competition between the reactions of metal cations and the pyrazolide anion and the BN adduct formation (Fig. 1). Another important factor which influences the stability of scorpionates is the degree of steric crowding. Several studies have shown that the scorpionates of the type $RB(3\text{-}R'pz)_3^-$ decompose in the presence of transition metal salts MX_n much more easily when R and R′ are bulky (Fig. 1) [10]. Especially scorpionates with pyrazoles which bear bulky substituents in 3- and 5-position tend to degradation. Therefore it is unfavorable to tune the properties of scorpionate ligands by introducing solubility-mediating or functionalized groups in their 3- or/and 5-position. Since our group has a long-standing interest in the development of new

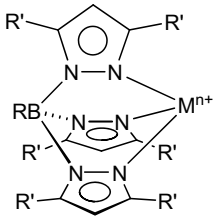

Fig. 1. Metal Scorpionates.

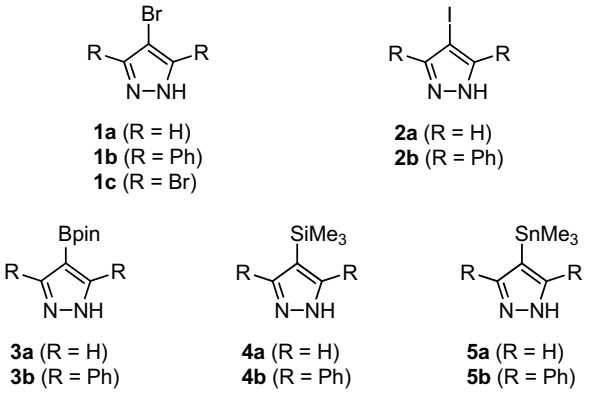

Fig. 2. The pyrazoles with their different functional groups in the 4-position.

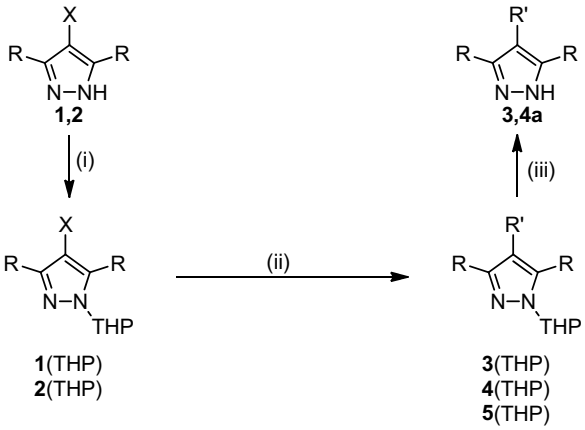

Scheme 1. Syntheses of the borylated, silylated and stannylated pyrazoles. (i) **1**, **2** (R = H, Ph; X = Br, I): toluene, +DHP; TFA, 95 °C (R = H, Ph; X = Br, I); (ii) **3a**, **b**(THP) (R′ = Bpin): *n*BuLi/*i*PrMgCl, +Bpin(O*i*Pr); **4a**(THP) (R′ = $SiMe_3$): +*n*BuLi, +Me_3SiCl; **5a**, **b**(THP) (R′ = $SnMe_3$): *n*BuLi/*i*PrMgCl +Me_3SnCl; THF, –78 °C, (iii) **3a**, **b** (R′ = Bpin), **4a** (R′ = $SiMe_3$): AcCl in MeOH; subsequent addition of NEt_3.

ligand systems based on pyrazole, both for use in homogeneous catalysis and in the assembly of coordination polymers and networks, we decided to work out a new strategy to introduce functional groups on pyrazoles. In the course of this study we found that pyrazole derivatives could conveniently be borylated, silylated or stannylated in the 4-position. Moreover, coupling protocols allow further functionalization of these pyrazoles.

The purpose of this paper is to describe the synthesis and properties of pyrazoles which bear functional groups in the 4-position (*c. f.* Fig. 2). In addition we examined microwave-assisted C–C cross-coupling reactions of these pyrazoles with aryl halides. Finally the solid-state structures of the pyrazoles **1b**, **3a**, **3b**, **4a**, and **5b**(THP) and those of the addition products of **1a** with HBr, **1c** with HBr, **1c** with HBr and Br_2, **2a** with H_2SO_4, and **3a** with H_2O are reported herein.

Results and Discussion

Due to their acidic protons, it is always necessary to transform parent pyrazoles into their THP derivatives before metalation in 4-position is carried out (*e. g.* with *n*BuLi). Therefore we worked out the following synthesis strategy for 4-boryl-, 4-silyl-, and 4-stannyl-substituted pyrazoles (Scheme 1): i) At first the bromo- and iodopyrazoles **1a**, **1b**, **2a**, and **2b** were reacted with 3,4-dihydro-2*H*-pyran to give the related THP-protected bromo- or iodopyrazole derivatives **1a**(THP), **1b**(THP), **2a**(THP), and **2b**(THP). ii) In a second step these THP derivatives were metalated by treatment with *n*BuLi or *i*PrMgCl. Subsequent reactions of the THP-protected metallopyrazoles 4-*M*-pz(THP) and 4-*M*-3,5-Ph_2pz(THP) (*M* = Li, MgBr) with Bpin(O*i*Pr), Me_3SiCl, and Me_3SnCl yielded **3a**(THP), **3b**(THP), **4a**(THP), **4b**(THP), **5a**(THP), and **5b**(THP). iii) Finally the THP derivatives **3a**(THP), **3b**(THP), and **4a**(THP) whose boryl and silyl substituents are inert against protic agents could be easily transformed into their parent pyrazoles **3a**, **3b**, and **4a** (Scheme 1). However, stannyl group elimination took place when the THP derivatives **5a**(THP) and **5b**(THP) were treated with HCl. Therefore we were not able to synthesize the deprotected pyrazoles **5a** and **5b**.

As shown in Scheme 2, Suzuki-type coupling protocols allow the further functionalization of the pyrazoles **1a**–**3b** (Fig. 2). We examined the following microwave-assisted C–C cross-coupling reactions in detail: Suzuki reactions of **3a** with *p*-

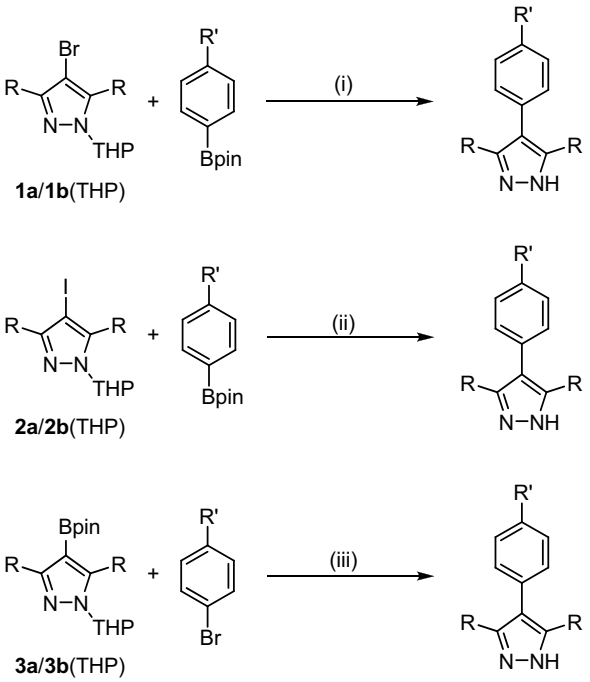

Scheme 2. Substituted pyrazoles **1**–**3** in C–C cross-coupling reactions. (i) *e. g.* **1b**(THP) (R = Ph), *p*-R′PhBpin (R′ = H) [9]; (ii) *e. g.* **2b**(THP) (R = Ph), *p*-R′PhBpin (R′ = Me) [13]; (iii) *e. g.* **3a**(THP) (R = H), *p*-R′PhBpin (R′ = pentyl): +Pd(PPh_3)$_4$, K_3PO_4, H_2O/DMF, 110 °C.

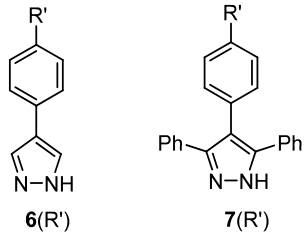

Fig. 3. Cross-coupling products **6**(R′) (*e. g.* R′ = pentyl, hexyl, 2-ethylhexyl, Ph [13]) and **7**(R′) (*e. g.* R′ = Me, Ph [13]).

pentylphenylbromide, *p*-hexylphenylbromide, and *p*-(2-ethylhexyl)phenylbromide.

In addition we performed Suzuki C–C cross-coupling reactions with the bromo- and iodo-substituted pyrazoles **1a**, **1b**, **2a**, and **2b** and pinacolatoboranes Ar-Bpin or aryl-substituted boronic acids ArB(OH)$_2$ (Fig. 3). In this context it should be noted that most of these C–C cross-coupling products are fluorophores and emit in the near ultraviolet to blue regime [13]. Moreover, some of these compounds show remarkably high solid-state quantum yields [13].

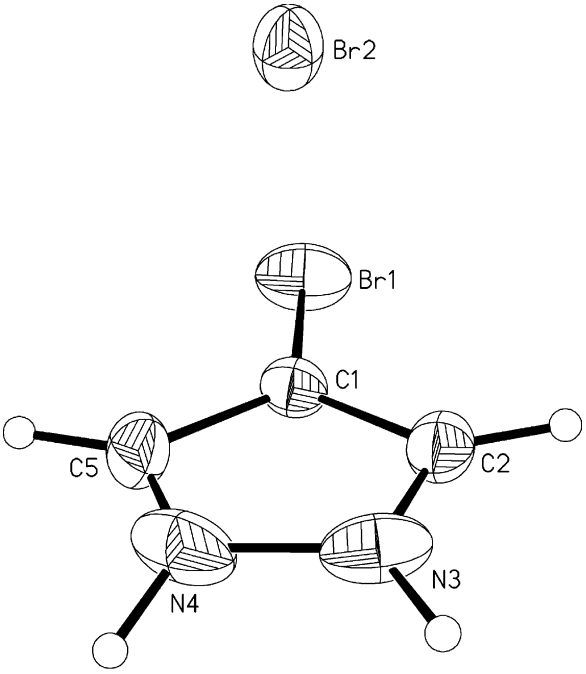

Fig. 4. Structure of **1a**·HBr in the solid state (ORTEP, displacement ellipsoids are drawn at the 50 % probability level). Selected bond lengths (Å), atom···atom distances (Å), and bond angles (deg): Br(1)–C(1) 1.854(6), C(1)–C(2) 1.381(9), C(1)–C(5) 1.383(9), C(2)–N(3) 1.321(9), N(3)–N(4) 1.320(10), N(3)–H(3) 0.89(1), N(4)–H(4) 0.89(1), N(4)–C(5) 1.305(10), N(3)···Br(2) 3.213(6), N(4)···Br(2) 3.258(6); N(3)–H(3)–Br(2) 131(7), N(4)–H(4)–Br(2) 147(7).

The molecular structures of the compounds **1a**·HBr, **1b**, (**1c**)$_2$·HBr, **1c**·HBr·(Br$_2$)$_{0.5}$, (**2a**)$_3$·H_2SO_4, **3a**, **3a**·H_2O, **3b**, **4a**, and **5b** are shown in Figs. 4 – 15. Selected bond lengths and angles are listed in the corresponding figure captions, details of the crystal structure analyses are summarized in Table 1.

The 1 : 1 addition product of **1a** and HBr crystallizes in the monoclinic space group $P2_1/n$ with $Z = 4$ (Fig. 4). The coordinates of the H atoms bonded to N were refined with a bond length restraint of 0.89(1) Å. The packing in the crystal shows layers of pyrazolium cations [**1a**H]$^+$ parallel to the (1 0 $\bar{4}$) plane and bromide anions. The bromide anion connects three cations by N–H···Br hydrogen bonds (N(3)–H(3) = 0.89(1) Å, N(3)···Br(2) = 3.213(6) Å, N(3)–H(3)–Br(2) = 131 (7)°, N(4)–H(4) = 0.89(1) Å, N(4)···Br(2) = 3.258(6) Å, N(4)–H(4)–Br(2) = 147 (7)°, N(3)–H(3) = 0.89(1) Å,

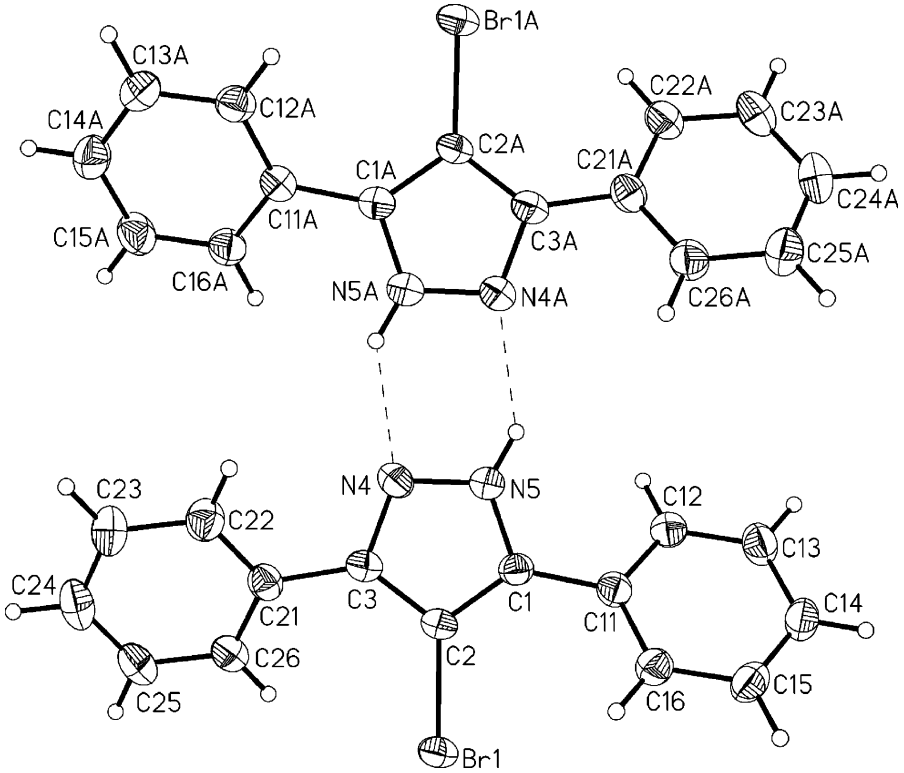

Fig. 5. Molecular structure of **1b** in the solid state (ORTEP, displacement ellipsoids are drawn at the 50% probability level). Selected bond lengths (Å), atom···atom distances (Å), bond angles (deg), and torsion angles (deg): Br(1)–C(2) 1.878(3), C(1)–N(5) 1.340(4), C(1)–C(2) 1.395(4), C(1)–C(11) 1.476(4), C(2)–C(3) 1.401(4), C(3)–C(4) 1.346(4), C(3)–N(21) 1.476(4), N(5)–H(5) 0.873(10), N(5A)–H(5A) 0.875(10), N(4)···N(5A) 2.827(4), N(5)···N(4A) 2.814(4); N(5)–H(5)–N(4A) 142(3), N(5A)–H(5A)–N(4) 142(3); pz(N(4))//Ph(C(11)) 35.25(12), pz(N(4))//Ph(C(21)) 31.09(13), pz(N(4A))//Ph(C(11A)) 31.90(12), pz(N(4A))//Ph(C(21A)) 27.80(15).

N(3)···Br(2) = 3.449(7) Å, N(3)–H(3)–Br(2) = 124 (6)°; Fig. 4). Thus, one of the H atoms (H(3)) forms two hydrogen bonds, whereas the other one forms just one.

The molecular structure of the pyrazole derivative **1b** (triclinic space group $P\bar{1}$ with $Z = 4$) is shown in Fig. 5. The coordinates of the H atoms bonded to N were refined with a bond length restraint of 0.88(1) Å. There are two molecules in the asymmetric unit differing in the dihedral angles between the central pyrazol ring and the attached phenyl rings. In the first molecule, the dihedral angles are 35.25(12)° and 31.09(13)° for the rings containing C(11) and C(21), respectively. In the second molecule, the dihedral angles are 31.90(12)° and 27.80(15)° for the rings containing C(11A) and C(21A), respectively. The two molecules in the asymmetric unit are connected by N–H···N hydrogen bonds to form dimers.

Two different addition products of 3,4,5-tribromopyrazole (**1c**) are shown in Figs. 6 and 7. The first one is composed of two molecules of **1c** and one of Br ((**1c**)$_2$·HBr) and the second one of one molecule each of **1c** and HBr, and a half molecule of Br_2 [**1c**·HBr·$(Br_2)_{0.5}$].

The H atoms in (**1c**)$_2$·HBr bonded to the N atoms were geometrically positioned and refined using a riding model. The position of the H atom bonded to the N(1) atom is only half-occupied. The asymmetric unit is composed of protonated pyrazole dimers $[(\mathbf{1c})_2H]^+$ and a bromide anion located on a two-fold axis. In the crystal, cations and bromide anions are connected *via* N–H···N and N–H···Br hydrogen bonds (N(1)–H(1) = 0.88 Å, N(1)···N(1) = 2.610(10) Å, N(1)–H(1)–N(1) = 175.8°, N(2)–H(2) = 0.88 Å, N(2)···Br(1) = 3.186(6) Å, N(2)–H(2)–Br(1) 166.1°; Fig. 7) forming zigzag chains running along the *a* axis.

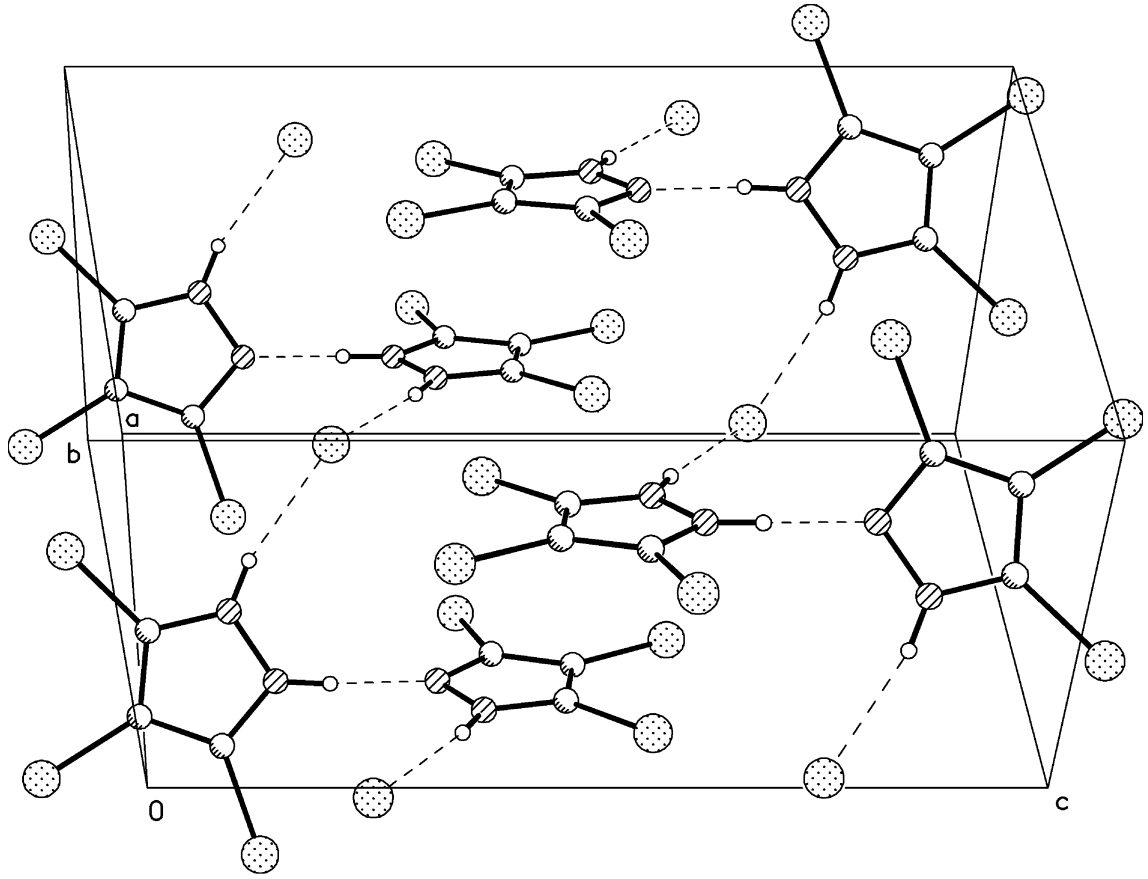

Fig. 6. Unit cell of $(\mathbf{1c})_2$·HBr.

The H atoms in **1c**·HBr·$(Br_2)_{0.5}$ bonded to the N atoms were geometrically positioned and refined using a riding model. The asymmetric unit is composed of one cation, one anion and half a Br_2 molecule which is located on a centre of inversion. In the crystal, two cations are connected to each other mediated by two bromide anions forming centrosymmetric dimers *via* N–H···Br hydrogen bonds (N(2)–H(2) = 0.88 Å, N(2)···Br(1) 3.180(6) Å, N(2)–H(2)–Br(1) = 161.8°, N(1)–H(1) = 0.88 Å, N(1)···Br(1) = 3.174(6) Å, N(1)–H(1)–Br(1) = 167.0°; Fig. 7). Anions and cations form layers in the (1 $\bar{2}$ 0) plane. The Br_2 molecules are located between the dimers. The shortest contact of a Br_2 molecule is to a bromide anion (3.0906(13) Å).

The H atoms bonded to the N atoms in $(\mathbf{2a})_3$·H_2SO_4 were freely refined with a bond length restraint of 0.88(1) Å for the bond N(2A)–H(2A). The asymmetric unit is composed of two protonated 4-iodo-pyrazolium cations $[\mathbf{2a}H]^+$, one 4-iodopyrazole molecule, and one sulfate anion. The neutral iodopyrazole molecule donates a hydrogen bond to a sulfate anion (N(1)–H(1) = 0.97(8) Å, N(1)···O(2) = 2.787(5) Å, N(1)–H(1)–O(2) = 158 (7)°) and accepts one hydrogen bond from a iodopyrazolium cation (N(2B)–H(2B) = 0.86(7) Å, N(2B)···N(2) = 2.678(6) Å, N(2B)–H(2B)–N(2) = 166(6)°). The other N–H group of this iodopyrazolium cation donates a hydrogen bond to a sulfate anion (N(1B)–H(1B) = 0.84(6) Å, N(1B)···O1 = 2.599(5) Å, N(1B)–H(1B)–O(1) = 172(6)°). The second iodopyrazolium cation connects two sulfate anions *via* N–H···O hydrogen bonds (N(1A)–H(1A) = 0.88(5) Å, N(1A)···O(4) = 2.631(5) Å, N(1A)–H(1A)–O(4) = 175(5)°, N(2A)–H(2A) = 0.88(2) Å, N(2A)···O(2) = 2.723(4) Å, N(2A)–H(2A)–O2 = 166(5)°). As a result, only three of the four sulfate O atoms act as hydrogen bond acceptors, whereas the N atom of the iodopyra-

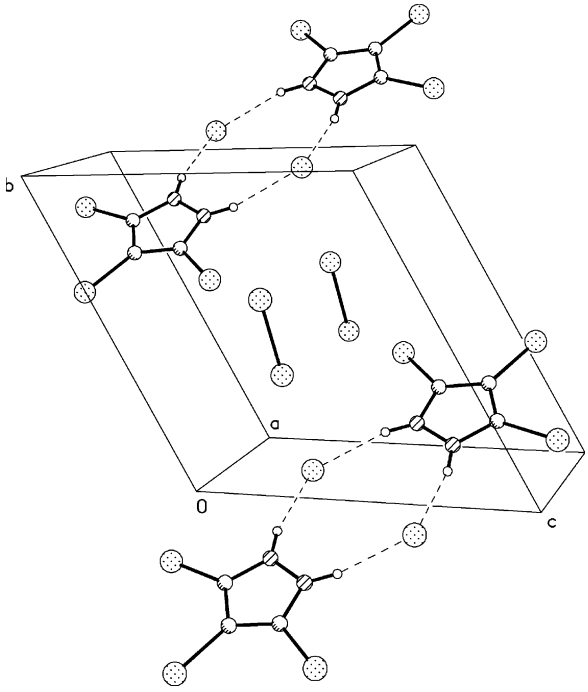

Fig. 7. Unit cell of **1c**·HBr·$(Br_2)_{0.5}$.

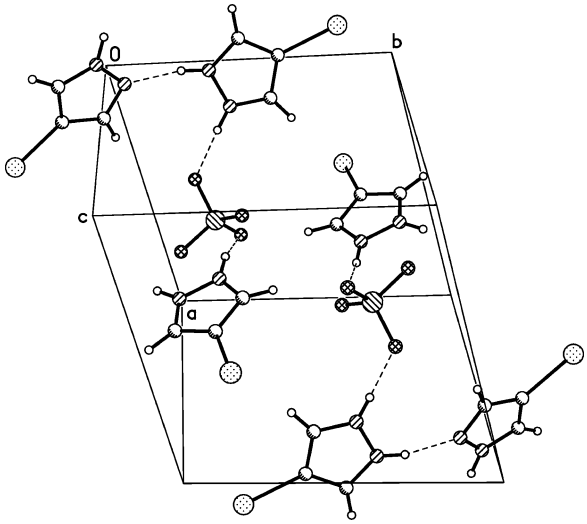

Fig. 8. Unit cell of $(\mathbf{2a})_3 \cdot H_2SO_4$.

zole molecule is involved in a N–H···N hydrogen bond. This hydrogen bond pattern leads to a two-dimensional arrangement of double layers in the *ab* plane (Fig. 8). However, there are no hydrogen bonds between these layers.

The molecular structure of the pyrazole **3a** (orthorhombic, space group $P2_12_12_1$ with $Z = 4$) is shown in Figs. 9 and 10. The H atom bonded to N was freely refined. The planar five-membered 1,3,2-dioxaborolane ring (r. m. s. deviation = 0.118 Å) is almost coplanar with the pyrazole ring (dihedral angle 8.98(13)°). In the crystal, the molecules are connected *via* N–H···N hydrogen bonds (N(2)–H(2) = 0.81(3) Å, N(2)···N(1) = 2.935(3) Å, N(2)–H(2)–N(1) = 166(3)°) to zigzag chains running along the *a* axis (Fig. 10). The molecules in this chain are coplanar and form ribbons in the (0 1 3) and (0 1 $\bar{3}$) planes.

The water O atom in **3a**·H_2O is located on a threefold rotation axis. The water H atoms are thus disordered over three positions with a site occupation factor of 2/3. The H atom bonded to the N atom is disordered over two positions with site occupation factors of 1/3 and 2/3 in accord with the disorder of the water H atoms. Due to the absence of anomalous scatterers, the absolute structure could not be determined. The planar five-membered 1,3,2-dioxaborolane ring (r. m. s. deviation = 0.124 Å) is almost coplanar with the pyrazole ring (dihedral angle = 8.06(6)°). In the crystal, three molecules are arranged about a threefold rotation axis surrounding the water molecule which is located on the threefold axis. The water molecule donates two hydrogen bonds to the N atoms of two pyrazole rings (O(1W)–H(1W) = 0.842(14) Å, O(1W)···N(4) = 2.885(3) Å, O(1W)–H(1W)–N(4) = 160(6)°), and the latter two donate an N–H bond to the N atom of the third molecule (N(3)–H(3) = 0.908(15) Å, N(3)···N(3) = 3.140(5) Å, N(3)–H(3)–N(3) = 142(7)°). This molecule donates an N–H bond to the water molecule (N(4)–H(4) = 0.909(15) Å, N(4)···O(1W) = 2.885(3) Å, N(4)–H(4)–O(1W) = 144(9)°) completing a tripodal arrangement of three molecules of pyrazole **3a** and a water molecule (Fig. 11). These complexes are not further connected *via* hydrogen bonds to symmetry-equivalent complexes.

The borylated pyrazole **3b** crystallizes with two molecules in the asymmetric unit in the orthorhombic space group $Pna2_1$ with $Z = 8$, as shown in Fig. 12. In one molecule, the dioxaborolane ring is disordered over two positions with a site occupation factor of 0.695(7) for the site of major occupancy. The disordered atoms were refined isotropically, while

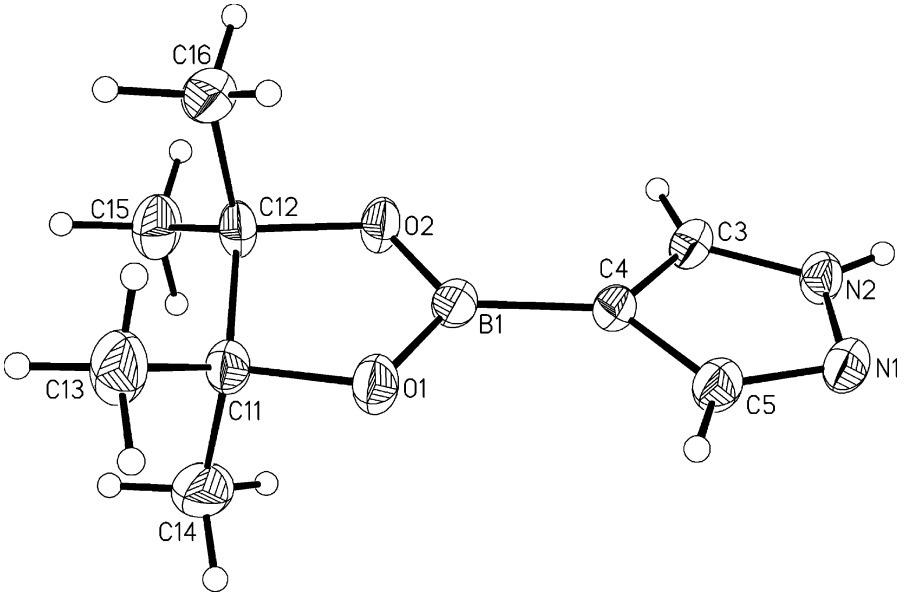

Fig. 9. Molecular structure of **3a** in the solid state (ORTEP, displacement ellipsoids are drawn at the 50 % probability level). Selected bond lengths (Å), atom···atom distances (Å), bond angles (deg), and torsion angles (deg): B(1)–C(4) 1.542(3), N(1)–C(5) 1.321(3), N(1)–N(2) 1.351(3), N(2)–C(3) 1.337(3), C(3)–C(4) 1.376(4), C(4)–C(5) 1.407(3), N(2)–H(2) 0.81(3), B(1)–C(4) 1.542(3), N(2)···N(1) 2.935(3); N(2)–H(2)–N1 166(3), pz(N(1))//Bpin(B(1)) 8.98(13).

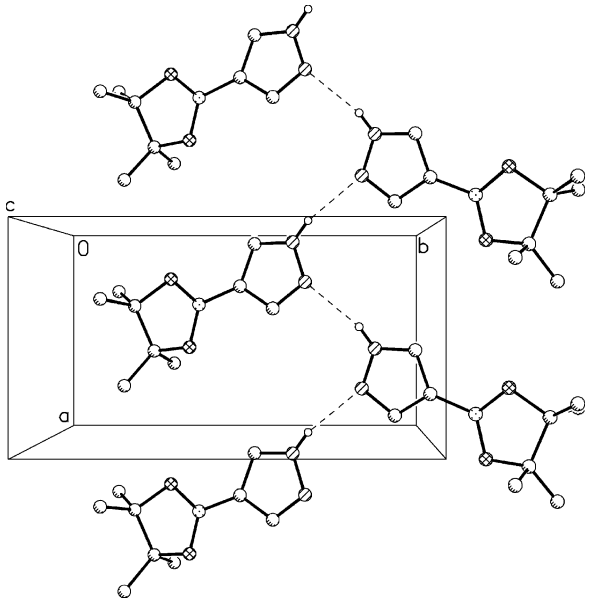

Fig. 10. Packing of borylated pyrazole molecules in crystals of **3a**, viewed in the *ab* plane. Hydrogen atoms except those on nitrogen atoms have been omitted for clarity.

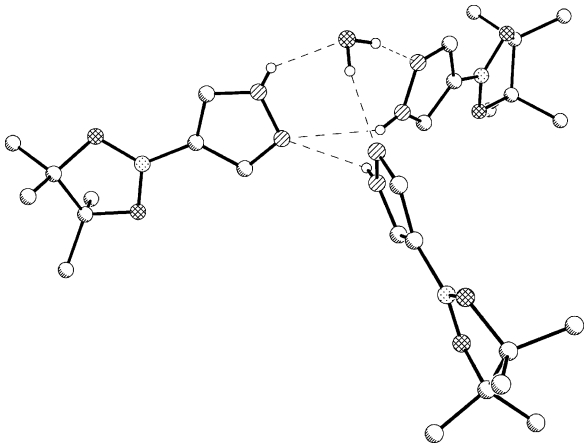

Fig. 11. Connectivity of $(\mathbf{3a})_3 \cdot H_2O$ in the solid state. Hydrogen atoms except those on nitrogen and oxygen atoms have been omitted for clarity.

the H atoms bonded to N were freely refined. Due to the absence of anomalous scatterers, the absolute structure could not be determined. The pyrazole ring containing N(1) forms dihedral angles of 39.39(10)° and 36.64(8)° with the phenyl ring containing C(21) and C(31), respectively. The pyrazole ring containing N(1A) forms dihedral angles of 38.85(11)° and 41.40(6)° with the phenyl rings containing C(21A) and C(31A), respectively. The two molecules in the asymmetric unit form dimers connected by

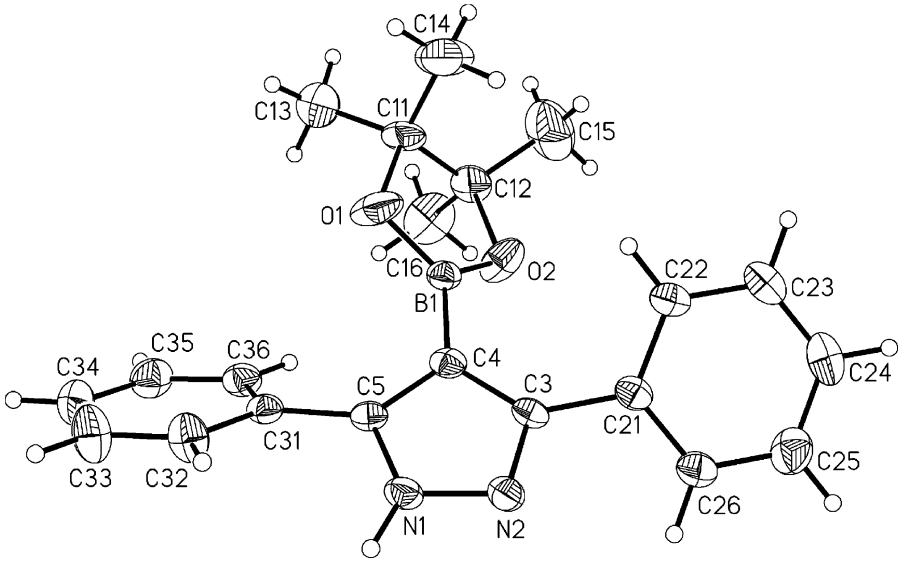

Fig. 12. Molecular structure of **3b** (ORTEP, displacement ellipsoids are drawn at the 50% probability level). Selected bond lengths (Å), atom···atom distances (Å), bond angles (deg), and torsion angles (deg): B(1)–C(4) 1.549(5), N(1)–C(5) 1.353(4), N(1)–N(2) 1.364(4), N(2)–C(3) 1.341(4), C(3)–C(4) 1.414(5), C(3)–C(21) 1.477(5), C(4)–C(5) 1.386(5), C(5)–C(31) 1.480(5), N(1)–H(1) 0.91(4), N(1A)–H(1A) 0.89(5), N(1)···N(2A) 2.926(4), N(2)···N(1A) 2.830(4); N(1)–H(1)–N(2A) 138(3), N(1A)–H(1A)–N(2) 147(4); pz(N(1))//Ph(C(21)) 39.39(10), pz(N(1))//Ph(C(31)) 36.64(8), pz(N(1A))//Ph(C(21A)) 38.85(11), pz(N(1A))//Ph(C(31A)) 41.40(6), pz(N(1))//pz(N(1A)) 34.43(10).

N–H···N hydrogen bonds (N(1)–H(1) = 0.91(3) Å, N(1)···N(1) = 2.926(4) Å, N(1)–H(1)–N(2A) = 138(3)°, N(1A)–H(1A) = 0.89(3) Å, N(1)···N(1A) = 2.830(4) Å, N(1)–H(1)–N(2A) = 147(3)°). The two hydrogen-bonded pyrazole rings are not coplanar but inclined at an angle of 34.43(10)°.

The molecular structure of the silylated pyrazole **4a** (monoclinic, space group *Pc* with $Z = 8$) is shown in Figs. 13 and 14. The three methyl groups in two molecules are disordered over two positions with site occupation factors of 0.55(6) and 0.78(2) for the site of major occupancy. Si–C and C–C bond lengths in the disordered parts were restrained to be equal to those in a non-disordered $SiMe_3$ group. One methyl C atom (C(6C)) was restrained to an isotropic behavior. The H atoms could not be located and were geometrically positioned. The absolute structure could not be reliably determined (Flack (*x*) parameter 0.8(5)). There are four molecules in the asymmetric unit, which are connected by N–H···N hydrogen bonds to zigzag chains running along the *b* axis (N(3)–H(3) = 0.88 Å, N(3)···N(4A) = 2.951(14) Å, N(3)–H(3)–N(4A) = 152, N(3A)–H(3A) = 0.88 Å, N(3A)···N(4B) = 2.850(15) Å, N(3A)–H(3A)–N(4B)

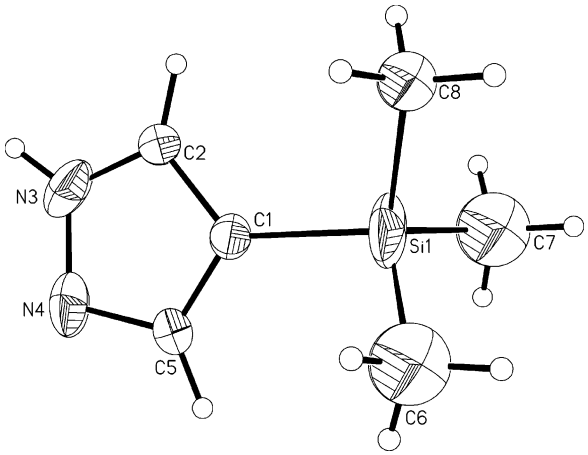

Fig. 13. Molecular structure of **4a** (ORTEP, displacement ellipsoids are drawn at the 50% probability level). Selected bond lengths (Å), atom···atom distances (Å), and bond angles (deg): C(1)–C(2) 1.395(18) Å, C(1)–C(5) 1.348(18), C(1)–Si(1) 1.860(12), C(2)–N(3) 1.316(18), N(3)–N(4) 1.379(19), N(4)–C(5) 1.377(16), N(3)–H(3) 0.88, N(3A)–H(3A) 0.88, N(3B)–H(3B) 0.88, N(3C)–H(3C) 0.88, N(3)···N(4A) 2.951(14), N(3A)···N(4B) 2.850(15), N(3B)···N(4C) 2.932(15), N(3C)···N(4) 2.828(17); N(3)–H(3)–N(4A) 152, N(3A)–H(3A)–N(4B) 169, N(3B)–H(3B)–N(4C) 148, N(3C)–H(3C)–N(4) 165.

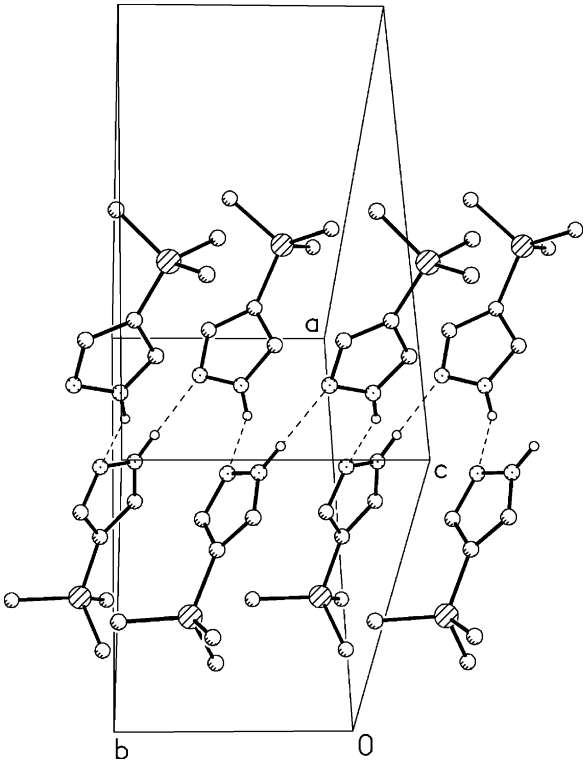

Fig. 14. Packing diagram for **4a**, viewed along the *ab* plane. Hydrogen atoms except those on nitrogen atoms have been omitted for clarity.

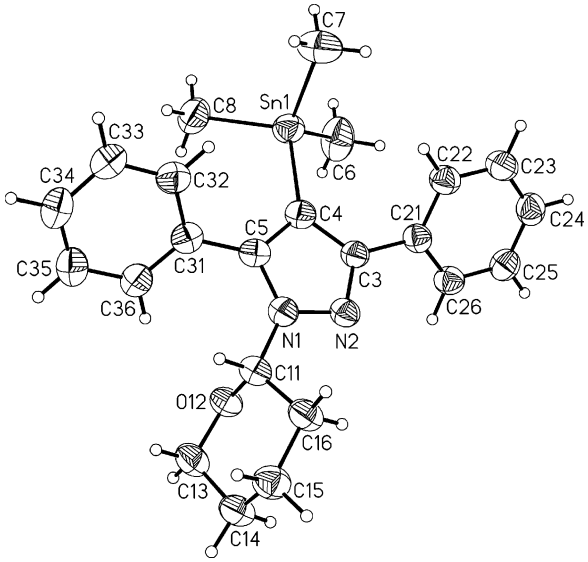

Fig. 15. Molecular structure of **5b**(THP) (ORTEP, displacement ellipsoids are drawn at the 50 % probability level). Selected bond lengths (Å) and torsion angles (deg): Sn(1)–C(4) 2.137(5), Sn(1)–C(6) 2.122(7), Sn(1)–C(7) 2.145(7), Sn(1)–C(8) 2.161(6), N(1)–N(2) 1.358(6), N(1)–C(5) 1.368(6), N(2)–C(3) 1.335(6), C(3)–C(4) 1.432(7), C(3)–C(21) 1.478(7), C(4)–C(5) 1.397(7), C(5)–C(31) 1.482(7); pz(N(1))//Ph(C(21)) 40.1(2), pz(N(1))//Ph(C(31)) 45.0(2).

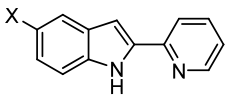

8(X)

Fig. 16. Pyridyl indoles (X = F, Cl).

= 169°, N(3B)–H(3B) = 0.88 Å, N(3B)···N(4C) = 2.932(15) Å, N(3B)–H(3B)–N(4C) = 148°, N(3C)–H(3C) = 0.88 Å, N(3C)···N(4) = 2.828(17) Å, N(3C)–H(3C)–N(4) = 165°; Fig. 14).

The stannylated pyrazole **5b**(THP) crystallizes in the monoclinic space group $P2_1/c$ with two almost identical molecules in the asymmetric unit (Fig. 15). A least-squares fit of all non-H atoms gives an r. m. s. deviation of 0.104 Å. Thus, only one molecule is discussed here. The pyrazole ring forms dihedral angles of 40.1(2)° and 45.0(2)° with the phenyl ring containing C(21) and C(31), respectively. The tetrahydropyranyl ring adopts a chair conformation. The Sn atom deviates by 0.381(9) Å from the plane of the pyrazole ring. The Sn–C bonds adopt typical values (Sn(1)–C(4) = 2.137(5) Å, Sn(1)–C(6) = 2.122(7) Å, Sn(1)–C(7) = 2.146(8) Å, Sn(1)–C(8) = 2.161(6) Å).

In summary, it was found that the crystal structures of herein described pyrazoles reveal two different types of hydrogen bonding networks in the solid state: infinite hydrogen-bridged zigzag chains of pyrazoles for small substituents in the 3- and 5-position (*e. g.* Fig. 2, R = H) and hydrogen-bridged dimers for bulky groups in these positions (*e. g.* Fig. 2, R = Ph). Also, it was found that proton-active compounds could easily be intercalated in this network. The pyrazole derivatives which are shown in Fig. 3 are excellent fluorophores and emit in the near ultraviolet to blue regime [13]. Moreover most of these compounds feature remarkable high solid-state quantum yields [13]. It is our current working hypothesis that the rigid framework of these pyrazoles, due to the hydrogen bonding networks in the solid state, prevents self-quenching. In contrast to these pyrazoles, despite of their strong fluorescence in dilute solutions, many related arenes, *e. g.*

Table 1. Crystal data and numbers pertinent to data collection and structure refinement of **1a** · HBr, **1b**, $(\mathbf{1c})_2$·HBr, **1c**·HBr·$(Br_2)_{0.5}$, $(\mathbf{2a})_3$·H_2SO_4, **3a**, **3a**·H_2O, **3b**, **4a**, and **5b**.

	1a·HBr	**1b**	$(\mathbf{2a})_3$·H_2SO_4
Formula	$C_3H_4Br_2N_2$	$C_{15}H_{11}BrN_2$	$C_9H_{11}I_3N_6O_4S$
M_r	227.90	299.17	680.00
Crystal size, mm^3	$0.60 \times 0.06 \times 0.03$	$0.20 \times 0.20 \times 0.10$	$0.43 \times 0.24 \times 0.17$
Crystal system	monoclinic	triclinic	triclinic
Space group	$P2_1/n$	$P\bar{1}$	$P\bar{1}$
a, Å	4.8444(8)	9.7718(7)	8.9930(8)
b, Å	7.2728(8)	9.8208(8)	9.3479(8)
c, Å	17.666(3)	13.3022(10)	11.1707(9)
α, deg	90	88.134(6)	77.945(7)
β, deg	97.711(13)	78.308(6)	89.325(7)
γ, deg	90	86.384(6)	82.048(7)
V, Å^3	616.79(16)	1247.34(17)	909.39(14)
Z	4	4	2
$D_{calcd.}$, g cm^{-3}	2.45	1.59	2.48
$\mu(\mathrm{Mo}K_\alpha)$, mm^{-1}	13.0	3.3	5.3
$F(000)$, e	424	600	628
hkl range	$\pm5, \pm8, \pm21$	$\pm12, -10/12, \pm16$	$\pm10, \pm11, \pm13$
$((\sin\theta)/\lambda)_{max}$, Å^{-1}	0.603	0.595	0.595
Refl. measured	7424	12804	13396
Refl. unique/R_{int}	1155/0.10	4909/0.08	3049/0.07
Param. refined	70	332	228
$R(F)/wR(F^2)$[a] (all refls.)	0.0520/0.1161	0.0527/0.1196	0.0320/0.0843
GoF (F^2)[a]	1.166	1.016	1.264
a/b[a]	0.0384/3.3504	0.0873/0	0.0321/1.9303
x (Flack)	–	–	–
$\Delta\rho_{fin}$ (max/min), e Å^{-3}	1.02/−1.19	0.99/−0.97	1.41/−0.98
	$(\mathbf{1c})_2$·HBr	**1c**·HBr·$(Br_2)_{0.5}$	**3a**
Formula	$C_6H_3Br_7N_4$	$C_3H_2Br_5N_2$	$C_9H_{15}BN_2O_2$
M_r	690.49	465.62	194.04
Crystal size, mm^3	$0.26 \times 0.09 \times 0.09$	$0.14 \times 0.12 \times 0.05$	$0.47 \times 0.07 \times 0.06$
Crystal system	monoclinic	triclinic	orthorhombic
Space group	$P2/c$	$P\bar{1}$	$P2_12_12_1$
a, Å	6.7961(8)	6.2262(7)	6.4338(5)
b, Å	8.5362(7)	9.7680(11)	11.6185(11)
c, Å	13.5242(17)	9.8982(12)	14.6384(15)
α, deg	90	115.824(8)	90
β, deg	97.497(10)	98.612(7)	90
γ, deg	90	90.796(7)	90
V, Å^3	777.87(15)	533.64(11)	1094.24(17)
Z	2	2	4
$D_{calcd.}$, g cm^{-3}	2.95	2.90	1.18
$\mu(\mathrm{Mo}K_\alpha)$, mm^{-1}	18.0	18.8	0.1
$F(000)$, e	624	418	416
hkl range	$\pm8, \pm10, \pm16$	$\pm7, \pm11, \pm12$	$\pm7, -14/13, \pm17$
$((\sin\theta)/\lambda)_{max}$, Å^{-1}	0.607	0.609	0.608
Refl. measured	9893	11694	13084
Refl. unique/R_{int}	1473/0.09	2001/0.07	1213/0.10
Param. refined	78	92	131
$R(F)/wR(F^2)$[a] (all refls.)	0.0482/0.0757	0.0568/0.1197	0.0489/0.1056
GoF (F^2)[a]	1.065	1.066	1.135
a/b[a]	0.0245/0	0.0436/1.6776	0.0594/0.1273
x (Flack)	–	–	3(2)
$\Delta\rho_{fin}$ (max/min), e Å^{-3}	0.60/−0.86	1.16/−1.02	0.20/−0.16

Table 1. (Continued.)

	(**3a**)$_3$·H$_2$O	**3b**	**4a**	**5b**(THP)
Formula	$C_9H_{15.67}BN_2O_{2.33}$	$C_{21}H_{23}BN_2O_2$	$C_6H_{12}N_2Si$	$C_{23}H_{28}N_2OSn$
M_r	200.04	346.22	140.27	467.16
Crystal size, mm^3	0.38 × 0.12 × 0.08	0.24 × 0.22 × 0.13	0.31 × 0.09 × 0.05	0.45 × 0.44 × 0.42
Crystal system	trigonal	orthorhombic	monoclinic	monoclinic
Space group	*R*3*c*	*Pna*2$_1$	*Pc*	*P*2$_1$/*c*
a, Å	21.9145(13)	14.0983(6)	14.738(2)	13.0408(7)
b, Å	21.9145(13)	17.751(11)	6.6246(13)	37.3306(14)
c, Å	12.2459(7)	15.3822(8)	19.942(3)	8.9951(5)
α, deg	90	90	90	90
β, deg	90	90	110.334(11)	90.687(4)
γ, deg	120	90	90	90
V, Å^3	5093.1(7)	3843.9(4)	1770.6(5)	4378.7(4)
Z	18	8	8	8
$D_{calcd.}$, g cm^{-3}	1.17	1.20	1.05	1.42
μ(MoK_α), mm^{-1}	0.1	0.1	0.2	1.2
F(000), e	1932	1472	608	1904
hkl range	±26, ±26, −13/15	±17, ±21, ±18	±18, ±7, ±24	±15, ±44, −10/9
$((\sin\theta)/\lambda)_{max}$, Å^{-1}	0.5905	0.595	0.595	0.595
Refl. measured	21745	44335	25234	33450
Refl. unique/R_{int}	2096/0.07	7400/0.10	6512/0.18	7739/0.10
Param. refined	142	474	321	487
$R(F)/wR(F^2)$[a] (all refls.)	0.0520/0.0850	0.0590/0.1328	0.1651/0.3216	0.0827/0.1464
GoF (F^2)[a]	1.102	1.067	0.999	1.132
a/b[a]	0.0436/0.4269	0.0722/0.8198	0.1952/0	0.0489/9.7047
x (Flack)	−0.8(6)	−0.8(9)	0.5(2)	–
$\Delta\rho_{fin}$ (max/min), e Å^{-3}	0.13/−0.13	0.51/−0.27	1.66/−0.48	0.85/−1.01

[a] $R(F) = \Sigma||F_o| - |F_c||/\Sigma|F_o|$; $wR(F^2) = [\Sigma w(F_o^2 - F_c^2)^2/\Sigma w(F_o^2)^2]^{1/2}$; GoF $= [\Sigma w(F_o^2 - F_c^2)^2/(n_{obs} - n_{param})]^{1/2}$; $w = [\sigma^2(F_o^2) + (aP)^2 + bP]^{-1}$, where $P = (\mathrm{Max}(F_o^2, 0) + 2F_c^2)/3$.

the pyridyl indols **8**(F) and **8**(Cl) (Fig. 16) [14], tend to show a poor performance in the solid state, mainly due to π stacking.

Experimental Section

The solvents THF, pentane, toluene, and C_6D_6 were stirred over sodium/benzophenone and distilled prior to use. **1a** [16], **1a**(THP) [17], **1b** [18], **1c** [19], **2a** [20], **2a**(THP) [21], **2b** [20], **3a** [22], **3a**(THP) [23], and **4a** [24] were prepared according to published procedures. All other starting materials were purchased from commercial sources and used without further purification. The NMR spectra were recorded on Bruker AM 250, DPX 250, Avance 400, and Avance 500 spectrometers. NMR chemical shifts are reported in ppm. Abbreviations: s = singlet; d = doublet; dd = doublet of doublets; t = triplet; m = multiplet; br = broad; n. o. = not observed. Mass spectrometry was performed with a Fisons VG Platform II instrument and microwave irradiation was generated with a Biotage Initiator$^+$ System. Elemental analyses were carried out by the Microanalytical Laboratory of the Goethe University Frankfurt.

*Crystals of 4-bromo-1H-pyrazole and HBr (**1a**·HBr)*

The bromopyrazole **1a** was prepared according to the published procedure [16]. By slow evaporation of the solvent water crystals of **1a** and HBr were grown from the reaction mixture at r. t.

*Single crystals of 4-bromo-3,5-diphenyl-1H-pyrazole (**1b**)*

The bromopyrazole **1b** was prepared according to the published procedure [18]. Single crystals of **1b** were grown from a CH_2Cl_2 solution by slow evaporation of the solvent at r. t.

*4-Bromo-3,5-diphenyl-1-THP-pyrazole (**1b**(THP))*

3,4-Dihydro-2*H*-pyran (DHP) (0.62 g, 7.35 mmol) was added dropwise at 85 °C to a mixture of **1b** (2.00 g, 6.69 mmol) and a catalytic amount of trifluoroacetic acid (TFA) (0.04 g, 0.33 mmol) in 20 mL toluene. The solution was warmed up to 95 °C and kept stirring for further 1 h. After removing all volatiles *in vacuo*, **1b**(THP) remained as a pale-yellow oil that was suitable for direct conversion (yield: 2.54 g, 99 %). – ^{1}H NMR (400 MHz, $CDCl_3$): δ = 7.98 – 7.95 (m, 2H, *o*Ph-H), 7.60 – 7.57 (m, 2H, *o*Ph-H), 7.55 – 7.50 (m, 3H, Ph-H), 7.46 – 7.42 (m, 2H, *m*Ph-H),

7.39 – 7.35 (m, 1H, *p*Ph-H), 5.14 (dd, J = 2.5, 10.1 Hz, 1H, THP-H), 4.14 – 4.10 (m, 1H, THP-H), 3.56 – 3.50 (m, 1H, THP-H), 2.65 – 2.55 (m, 1H, THP-H), 2.10 – 2.06 (m, 1H, THP-H), 1.87 – 1.83 (m, 1H, THP-H), 1.79 – 1.69 (m, 1H, THP-H), 1.61 – 1.50 (m, 2H, THP-H). – ^{13}C NMR (100 MHz, $CDCl_3$): δ = 149.0 (pzC-3,5), 143.4 (pzC-3,5), 132.5 (Ph*C*), 130.4 (Ph*C*H), 129.5 (Ph*C*H), 128.7 (Ph*C*H), 128.4 (Ph*C*H), 128.3 (Ph*C*H), 128.3 (Ph*C*H), 93.6 (pzC-4), 85.2 (THP), 67.9 (THP), 29.5 (THP), 24.9 (THP), 22.9 (THP), n. o. (Ph*C*).

*Single crystals of (**1c**)$_2$·HBr and **1c**·HBr·(Br$_2$)$_{0.5}$*

The bromopyrazole **1c** was prepared according to the published procedure [19]. Single crystals of (**1c**)$_2$·HBr were grown from the reaction mixture at r. t. In a second crop crystals containing **1c**, HBr, and Br_2 in the ratio of 1 : 1 : 0.5 were obtained from this solution at r. t.

*Crystals of 4-iodo-1H-pyrazole and H_2SO_4 ((**2a**)$_3$·H_2SO_4)*

The iodopyrazole **2a** was prepared according to the published procedure [20]. By slow evaporation of the solvent crystals of (**2a**)$_3$·H_2SO_4 were grown from a chloroform solution at r. t.

*Single crystals of 4-iodo-3,5-diphenyl-1H-pyrazole (**2b**)*

The iodopyrazole **2b** was prepared according to the published procedure [20]. Single crystals of **2b** were grown from a $CHCl_3$ solution by slow evaporation of the solvent at r. t.

*4-Iodo-3,5-diphenyl-1-THP-pyrazole (**2b**(THP))*

2b(THP) was synthesized following the same procedure as described for **1b**(THP) from DHP (0.13 g, 1.59 mmol), **2b** (0.50 g, 1.44 mmol), TFA (0.01 g, 0.07 mmol) and 10 mL toluene. Pale-yellow oil (yield: 0.61 g, 98 %). – ^{1}H NMR (400 MHz, $CDCl_3$): δ = 7.92 – 7.90 (m, 2H, *o*Ph-H), 7.56 – 7.50 (m, 5H, Ph-H), 7.47 – 7.43 (m, 2H, *m*Ph-H), 7.40 – 7.38 (m, 1H, *p*Ph-H), 5.12 (dd, J = 2.5, 10.1 Hz, 1H, THP-H), 4.12 – 4.08 (m, 1H, THP-H), 3.53 – 3.47 (m, 1H, THP-H), 2.63 – 2.51 (m, 1H, THP-H), 2.08 – 2.04 (m, 1H, THP-H), 1.87 – 1.83 (m, 1H, THP-H), 1.79 – 1.68 (m, 1H, THP-H), 1.60 – 1.49 (m, 2H, THP-H). – ^{13}C NMR (100 MHz, $CDCl_3$): δ = 152.3 (pzC-3,5), 146.8 (pzC-3,5), 133.2 (Ph*C*), 130.7 (Ph*C*H), 129.9 (Ph*C*), 129.5 (Ph*C*H), 128.8 (Ph*C*H), 128.7 (Ph*C*H), 128.3 (Ph*C*H), 128.2 (Ph*C*H), 85.4 (THP), 67.9 (THP), 62.3 (pzC-4), 29.6 (THP), 24.9 (THP), 22.9 (THP).

*Single crystals of 4-pinacolatoboryl-1H-pyrazole (**3a**)*

The pyrazole **3a** was prepared according to the published procedure [22]. Single crystals of **3a** were grown from an ethyl acetate solution by slow evaporation of the solvent at r. t.

*Crystals of 4-pinacolatoboryl-1H-pyrazole and H_2O ((**3a**)$_3$·H_2O)*

The pyrazole **3a** was prepared according to the published procedure [22]. By slow evaporation of the solvent water crystals of (**3a**)$_3$·H_2O were grown from the reaction solution at r. t.

*4-Pinacolatoboryl-3,5-diphenyl-1H-pyrazole (**3b**)*

A 2 M solution of *i*PrMgCl (0.31 g, 3.03 mmol) was added dropwise to a cooled (−4 °C) solution of **2b**(THP) (0.87 g, 2.02 mmol) in THF (10 mL). After 15 min (Bpin)O*i*Pr (1.13 g, 6.07 mmol) was added dropwise at −4 °C to the suspension. The resulting mixture was stirred for further 1.5 h and slowly warmed up to r. t. overnight. After the addition of saturated aqueous NH_4Cl solution, the slurry was diluted with toluene (25 mL) and washed with brine (3 × 20 mL). The organic layer was dried over anhydrous $MgSO_4$. After removal of all volatile compounds *in vacuo*, a yellow oil was obtained. **3b**(THP) was treated with 20 mL of a methanolic HCl solution (AcCl in MeOH) and stirred for 30 min. After the addition of NEt_3 (2 mL), the solution was stirred for further 30 min, diluted with Et_2O (50 mL), washed with water (3 × 30 mL), and dried over anhydrous $MgSO_4$. Evaporation of the solvents gave a yellow oil, which was purified by column chromatography (hexane/ethyl acetate 3 : 1). Single crystals were grown by gas-phase diffusion of cyclohexane into a solution of **3b** in benzene. Colorless solid (yield: 0.52 g, 60 %). – ^{1}H NMR (500 MHz, $CDCl_3$): δ = 7.73 – 7.71 (m, 4H, *o*Ph-H), 7.43 – 7.36 (m, 6H, Ph-H), 1.26 (s, 12H, CH_3), n. o. (N-H). – ^{13}C NMR (126 MHz, $CDCl_3$): δ = 154.6 (pzC-3,5), 132.5 (Ph*C*), 128.6 (Ph*C*H), 128.5 (Ph*C*H), 128.4 (Ph*C*H), 83.8 (*C*CH_3), 24.9 (CH_3). – ^{11}B{H} NMR (160 MHz, $CDCl_3$): δ = 31.3 ($h_{1/2}$ = 350 Hz). – MS ((+)-ESI): m/z(%) = 347.6 (100) $[M+H]^+$. – $C_{21}H_{23}BN_2O_2$ (346.2): calcd. C 72.85, H 6.70, N 8.09; found C 73.41, H 6.68, N 7.47.

*4-Trimethylsilyl-1H-pyrazole (**4a**)*

The pyrazole **4a** was synthesized from **4a**(THP) following the same procedure as described for **3a** and **3b**. The THP-protected iodopyrazole **2a**(THP) [21] (0.20 g, 0.72 mmol), *n*BuLi (0.12 g, 1.80 mmol), and Me_3SiCl (0.23 g, 2.16 mmol) were used as starting materials. – ^{1}H NMR (250 MHz, C_6D_6): δ = 7.81 (s, 1H, pzH-3,5), 7.28 (s, 1H, pzH-3,5), 5.68 (dd, J = 3.2, 9.1 Hz, 1H, THP-H), 4.10 – 4.04 (m, 1H, THP-H), 3.84 – 3.67 (m, 1H, THP-H), 2.63 – 2.51 (m, 1H, THP-H), 2.08 – 2.04 (m, 1H, THP-H), 1.87 – 1.83 (m, 1H, THP-H), 1.79 – 1.68 (m, 1H, THP-H), 1.60 – 1.49 (m, 2H, THP-H), 0.15 (s, 9H, CH_3). After treat-

ment of **4a**(THP) with 20 mL of a methanolic HCl solution (AcCl in MeOH) **4a** was obtained. Spectroscopic data see ref. [24].

An alternative and more convenient synthesis of **4a**: 4-Bromo-1*H*-pyrazole (6.69 g, 45.52 mmol) was dissolved in 50 mL THF and the solution was cooled to −78 °C. This solution was treated dropwise with a 1.6 M *n*BuLi solution in hexane (5.83 g, 91.04 mmol). The reaction mixture was subsequently stirred for 1 h at 0 °C. Me_3SiCl (14.02 g, 129.05 mmol) was added dropwise at −78 °C. The reaction mixture was warmed up to r. t. overnight. Then it was quenched with an aqueous NaOH solution, diluted with ethyl acetate (150 mL) and washed with a saturated $NaHCO_3$ solution (3 × 50 mL). The crude product was purified by column chromatography (hexane/ethyl acetate 2 : 1) to yield colorless crystals (yield: 2.19 g, 60 %). Spectroscopic data see ref. [24].

*4-Trimethylsilyl-3,5-diphenyl-1-THP-pyrazole (**4b**(THP))*

The pyrazole **4b**(THP) was synthesized following the same procedure as described for **3a**(THP), **3a**(THP), and **4a**(THP). The THP-protected iodopyrazole **2b**(THP) [21] (0.20 g, 0.52 mmol), *n*BuLi (0.08 g, 1.30 mmol), and Me_3SiCl (0.17 g, 1.57 mmol) were used as starting materials. – ^{1}H NMR (250 MHz, C_6D_6): δ = 7.86 – 7.82 (m, 2H, *o*Ph-H), 7.30 – 7.10 (m, 8H, Ph-H), 5.04 (dd, J = 3.2, 9.6 Hz, 1H, THP-H), 3.88 – 3.84 (m, 1H, THP-H), 3.16 – 3.06 (m, 1H, THP-H), 2.87 – 2.68 (m, 1H, THP-H), 1.74 – 1.61 (m, 2H, THP-H), 1.37 – 1.26 (m, 1H, THP-H), 1.07 – 0.88 (m, 2H, THP-H), −0.01 (s, 9H, CH_3).

*4-Trimethylsilyl-3,5-diphenyl-1-TMS-pyrazole (**4b**(TMS))*

4-Bromo-3,5-diphenyl-1*H*-pyrazole (0.40 g, 1.34 mmol) was dissolved in 10 mL THF, and the solution was cooled to −78 °C. This solution was treated dropwise with a 1.52 M *n*BuLi solution in hexane (0.21 g, 3.34 mmol). The reaction mixture was subsequently stirred for 1 h at 0 °C. Me_3SiCl (0.43 g, 4.01 mmol) was added dropwise at −78 °C. The reaction mixture was warmed up to r. t. overnight. NMR data were collected without further purification. Colorless solid (yield: 0.95 g, 72 %). – ^{1}H NMR (500 MHz, C_6D_6): δ = 7.85 – 7.83 (m, 2H, *o*Ph-H), 7.29 – 7.27 (m, 2H, *o*Ph-H), 7.24 – 7.21 (m, 2H, *m*Ph-H), 7.18 – 7.14 (m, 1H, *p*Ph-H), 7.10 – 7.03 (m, 3H, Ph-H), 0.19 (s, 9H, $NSiCH_3$), 0.00 (s, 9H, $CSiCH_3$). – ^{13}C NMR (125 MHz, C_6D_6): δ = 161.3 (pzC-3,5), 156.9 (pzC-3,5), 137.7 (Ph*C*), 135.3 (Ph*C*), 131.2 (Ph*C*H), 130.1 (Ph*C*H), 128.9 (Ph*C*H), 128.4 (Ph*C*H), 128.2 (Ph*C*H), 128.0 (Ph*C*H), 113.8 (pzC-4), 1.2 ($CSiCH_3$), 0.9 ($NSiCH_3$). – ^{29}Si NMR (99 MHz, C_6D_6): δ = 15.4, −10.9.

*4-Trimethylstannyl-1-THP-pyrazole (**5a**(THP))*

A 1.52 M *n*BuLi solution in hexane (0.14 g, 2.20 mmol) was added dropwise (−78 °C) to a stirred solution of **1a**(THP) (0.39 g, 1.70 mmol) in THF (6 mL). After stirring at −78 °C for 2 h, a solution of Me_3SnCl (0.50 g, 2.53 mmol) in THF (5 mL) was added dropwise to the cooled reaction mixture (−78 °C). The suspension was warmed to r. t. overnight, then diluted with Et_2O (60 mL) and treated with water (60 mL). The organic layer was dried over anhydrous $MgSO_4$ and evaporated to dryness *in vacuo*. However, the synthesis of **5a**(THP) was not quantitative. Beside the main product **5a**(THP) we observed two other stannylated and THP-protected pyrazol derivatives, namely 3-Me_3Sn-pz(THP) and 5-Me_3Sn-pz(THP) (ratio in the ^{1}H NMR spectrum: ∼65 % for **5a**(THP), ∼25 % for 3-Me_3Sn-pz(THP), ∼10 % for 5-Me_3Sn-pz(THP)). Spectroscopic data for **5a**(THP): – ^{1}H NMR (500 MHz, $CDCl_3$): δ = 7.53 (s, 1H, pzH-3,5), 7.51 (s, 1H, pzH-3,5), 5.42 (dd, J = 2.3, 10.0 Hz, 1H, THP-H), 4.09 – 4.06 (m, 1H, THP-H), 3.73 – 3.68 (m, 1H, THP-H), 2.21 – 2.13 (m, 1H, THP-H), 2.09 – 2.04 (m, 2H, THP-H), 1.74 – 1.66 (m, 3H, THP-H), −0.19 (s, 9H, CH_3). – ^{13}C NMR (125 MHz, $CDCl_3$): δ = 145.6 (pzC-3,5), 132.8 (pzC-3,5), 111.7 (pzC-4), 87.5 (THP), 68.1 (THP), 30.8 (THP), 25.2 (THP), 22.8 (THP), −9.1 (CH_3).

*4-Trimethylstannyl-3,5-diphenyl-1-THP-pyrazole (**5b**)*

1b(THP) (1.09 g, 2.84 mmol) in THF (15 mL) was treated dropwise with a 1.35 M *n*BuLi solution in hexane (0.24 g, 3.70 mmol) at −78 °C and stirred for 2 h. A solution of Me_3SnCl (0.85 g, 4.27 mmol) in THF (10 mL) was added dropwise to the cooled reaction mixture (−78 °C). After warming up to r. t. overnight, the suspension was diluted with Et_2O (100 mL) and treated with water (150 mL). The organic layer was dried over anhydrous $MgSO_4$ and concentrated to a volume of 2 mL. The product precipitated after 12 h. Analytically pure **5** was obtained from the crude product by washing with hexane. Single crystals were grown by slow evaporation of a $CDCl_3$ solution. Colorless solid (yield: 0.95 g, 72 %). – ^{1}H NMR (250 MHz, $CDCl_3$): δ = 7.64 – 7.59 (m, 2H, *o*Ph-H), 7.47 (s, 5H, Ph-H), 7.42 – 7.33 (m, 3H, Ph-H), 5.10 (dd, J = 2.4, 10.3 Hz, 1H, THP-H), 4.14 – 4.08 (m, 1H, THP-H), 3.55 – 3.45 (m, 1H, THP-H), 2.69 – 2.53 (m, 1H, THP-H), 2.07 – 2.01 (m, 1H, THP-H), 1.90 – 1.85 (m, 1H, THP-H), 1.79 – 1.46 (m, 3H, THP-H), −0.19 (s, 9H, CH_3). – ^{13}C NMR (63 MHz, $CDCl_3$): δ = 158.7 (pzC-3,5), 151.0 (pzC-3,5), 136.2 (Ph*C*), 132.5 (Ph*C*), 130.4 (Ph*C*H), 128.9 (Ph*C*H), 128.8 (Ph*C*H), 128.5 (Ph*C*H), 128.2 (Ph*C*H), 127.7 (Ph*C*H), 112.1 (pzC-4), 84.6 (THP), 67.9 (THP), 30.0 (THP), 25.0 (THP), 23.1 (THP), −8.0 (CH_3). – MS ((+)-ESI): m/z(%) = 469.2 (100) $[M+H]^+$. – $C_{23}H_{28}N_2OSn$ (467.2): calcd. C 59.13, H 6.04, N 6.00; found C 58.98, H 6.12, N 5.98.

*4-(p-Pentylphenyl)-1H-pyrazole (**6**(pentyl)) [13]*

K_3PO_4 (0.33 g, 1.54 mmol) was dissolved in 5 mL dmf and 5 mL water, and the solution was saturated with argon. A mixture of $Pd(PPh_3)_4$ (0.06 g, 0.05 mmol), **3a**(THP) (0.14 g, 0.51 mmol), and 4-pentylbromobenzene (0.12 g, 92 μL, 0.51 mmol) was added to the K_3PO_4 solution. The resulting suspension was saturated with argon. After microwave irradiation at 120 °C for 20 min, the reaction mixture was treated with a saturated aqueous $NaHCO_3$ solution (30 mL). The product was extracted into ethyl acetate (3 × 30 mL). The combined organic layers were washed three times with 30 mL of a saturated aqueous NaCl solution and dried over anhydrous $MgSO_4$. After removal of the solvent *in vacuo*, the THP-protected product remained as a pale-yellow oil (0.12 g, 82 %). Treatment with a solution of HCl in MeOH (10 mL, AcCl in MeOH) and stirring for 30 min yielded the hydrochloride of **6**(pentyl) [13]. When the hydrochloride was treated with NEt_3 (1 mL), the pyrazole **6**(pentyl) [13] was obtained quantitatively. After evaporation of the solvent, the crude product was purified by column chromatography (hexane/ethyl acetate 2 : 1). Colorless solid (yield: 0.07 g, 68 %). – ^{1}H NMR (500 MHz, CD_3OD): δ = 7.90 (br, 2H, pzH-3,5), 7.46 (d, 2H, J = 8.0 Hz, Ph-H), 7.17 (d, 2H, J = 8.0 Hz, Ph-H), 2.60 (t, 2H, J = 7.6 Hz, CH_2), 1.66 – 1.60 (m, 2H, CH_2), 1.38 – 1.29 (m, 4H, 2 × CH_2), 0.91 (t, 3H, J = 7.0 Hz, CH_3), n. o. (N-H). – ^{13}C NMR (126 MHz, CD_3OD): δ = 142.2 (Ph*C*), 137.3 (pzC-3,5), 131.4 (Ph*C*), 129.9 (Ph*C*H), 126.5 (Ph*C*H), 123.7 (pzC-4), 36.5 (CH_2), 32.6 (CH_2), 32.4 (CH_2), 23.6 (CH_2), 14.4 (CH_3). – MS ((+)-ESI): m/z(%) = 215.9 (13) $[M+H]^+$.

*4-(p-Hexylphenyl)-1H-pyrazole (**6**(hexyl)) [13]*

6(hexyl) [13] was synthesized following the same procedure as for **6** from K_3PO_4 (0.34 g, 1.62 mmol), $Pd(PPh_3)_4$ (0.06 g, 0.05 mmol), **3a**(THP) (0.15 g, 0.54 mmol), and 4-hexylbromobenzene (0.13 g, 0.54 mmol). Colorless solid (yield: 0.11 g, 65 %). – ^{1}H NMR (500 MHz, CD_3OD): δ = 7.90 (s, 2H, pzH-3,5), 7.45 (d, 2H, J = 8.0 Hz, Ph-H), 7.15 (d, 2H, J = 8.0 Hz, Ph-H), 2.60 (t, 2H, J = 7.5 Hz, CH_2), 1.66 – 1.58 (m, 2H, CH_2), 1.38 – 1.29 (m, 6H, 3x CH_2), 0.91 – 0.88 (m, 3H, CH_3), n. o. (N-H). – ^{13}C NMR (126 MHz, CD_3OD): δ = 142.2 (Ph*C*), 133.1 (pzC-3,5), 131.4 (Ph*C*), 129.9 (Ph*C*H), 126.5 (Ph*C*H), 123.7 (pzC-4), 36.5 (CH_2), 32.6 (CH_2), 32.4 (CH_2), 25.0 (CH_2), 23.6 (CH_2), 14.4 (CH_3). – MS ((+)-ESI): m/z(%) = 229.8 (100) $[M+H]^+$.

*4-(p-(2-Ethylhexyl)phenyl)-1H-pyrazole (**6**(2-ethylhexyl)) [13]*

6(2-ethylhexyl) [13] was synthesized following the same procedure as for **6**(pentyl) [13] from K_3PO_4 (0.82 g, 3.86 mmol), $Pd(PPh_3)_4$ (0.15 g, 0.12 mmol), **3a**(THP) (0.36 g, 1.29 mmol), and 4-(2-ethylhexyl)bromobenzene (0.35 g, 1.29 mmol). Colorless solid (yield: 0.29 g, 65 %). – ^{1}H NMR (250 MHz, CD_3OD): δ = 7.90 (s, 2H, pzH-3,5), 7.47 (d, 2H, J = 8.3 Hz, Ph-H), 7.14 (d, 2H, J = 8.3 Hz, Ph-H), 2.53 (d, 2H, J= 7.0 Hz, CH_2), 1.62 – 1.52 (m, 1H, CH), 1.35 – 1.24 (m, 8H, 4 × CH_2), 0.93 – 0.87 (m, 6H, 2 × CH_3), n. o. (N-H). – ^{13}C NMR (63 MHz, CD_3OD): δ = 141.1 (Ph*C*), 131.4 (Ph*C*), 130.7 (Ph*C*H), 126.4 (Ph*C*H), 123.8 (pzC-4), 42.5 (CH), 40.8 (CH_2), 33.5 (CH_2), 30.0 (CH_2), 26.6 (CH_2), 24.0 (CH_2), 14.4 (CH_3), 11.2 (CH_3), n. o. (pzC-3,5). – MS ((+)-ESI): m/z(%) = 258.3 (100) $[M+H]^+$. – $C_{17}H_{24}N_2$ (256.4): calcd. C 79.64, H 9.44, N 10.33; found C 79.28, H 9.29, N 9.81.

Crystal structure determinations

Data for (**1c**)$_2$·HBr and **1c**·HBr·$(Br_2)_{0.5}$ were collected on a Stoe IPDS II two-circle diffractometer with graphite-monochromated MoK_α radiation (λ = 0.71073 Å) and corrected for absorption with an empirical absorption correction using the program PLATON [25]. Data for **1a**·HBr, **1b**, (**2a**)$_3$·H_2SO_4, **3a**, (**3a**)$_3$·H_2O, **3b**, **4a**, and **5b**(THP) were collected on a Stoe IPDS II two-circle diffractometer with a Genix Microfocus tube with mirror optics using MoK_α radiation (λ = 0.71073 Å) and were scaled using the frame scaling procedure in the X-AREA program system [26]. The structures were solved by Direct Methods using the program SHELXS [27] and refined against F^2 with full-matrix least-squares techniques using the program SHELXL-97 [27].

The H atoms bonded to the N atoms in **1c**·HBr·$(Br_2)_{0.5}$ and (**1c**)$_2$·HBr were geometrically positioned and refined using a riding model. The H atom bonded to the N(1) atom has an occupation factor of 0.5.

The coordinates of the H atoms bonded to N in **1a**·HBr were refined restraining the N–H bond lengths to 0.89(1) Å. The H atoms bonded to B in **3a** were isotropically refined. Due to the absence of anomalous scatterers, the absolute structure of **3a** could not be determined. The coordinates of the H atoms bonded to N and O in (**3a**)$_3$·H_2O were refined restraining the O–H bond lengths to 0.84(1) Å and the N–H bond lengths to 0.91(1) Å. The H atoms bonded to O and N(3) have a site occupation factor of 2/3 and the H atom bonded to N(4) has a site occupation factor of 1/3. Due to the absence of anomalous scatterers, the absolute structure of (**3a**)$_3$·H_2O could not be determined.

In **4a** the three methyl groups of two molecules are disordered over two positions with site occupation factors of 0.55(6) and 0.78(2) for the site with the major occupancy. Si–C and C–C bond lengths in the disordered parts were restrained to be equal to those in a non-disordered $SiMe_3$ group. The disordered atoms were refined isotropically. One methyl C atom (C(6C)) was restrained to an isotropic behav-

ior. The H atoms could not be located and were geometrically positioned. The absolute structure could not be reliably determined, Flack (*x*) parameter 0.8(5). Attempts to refine the structure in the space group $P2_1/c$ failed.

The H atoms bonded to N in (**1a**)$_3$·H_2SO_4 were isotropically refined restraining the N(2A)–H(2A) bond length to 0.88(1) Å.

In one molecule of **3b**, the dioxaborolane ring is disordered over two positions with a factor of 0.695(7) for the site with the major occupancy. The disordered atoms were refined isotropically. The H atoms bonded to N were freely refined. Due to the absence of anomalous scatterers, the absolute structure could not be determined. The coordinates of the H atoms bonded to the N atoms in **1b** were refined restraining the N–H bond lengths to 0.88(1) Å.

CCDC 954167 (**1a**·HBr), CCDC 954174 (**1b**), CCDC 954166 ((**1c**)$_2$·HBr), CCDC 954165 (**1c**·HBr·$(Br_2)_{0.5}$), CCDC 954171 ((**2a**)$_3$·H_2SO_4), CCDC 954168 (**3a**), CCDC 954169 ((**3a**)$_3$·H_2O), CCDC 954172 (**3b**), CCDC 954170 (**4a**), and CCDC 954173 (**5b**(THP)) contain the supplementary crystallographic data for this paper. These data can be obtained free of charge from The Cambridge Crystallographic Data Centre *via* www.ccdc.cam.ac.uk/data_request/cif.

[1] S. Trofimenko, *Scorpionates – The Coordination Chemistry of Polypyrazolylborate Ligands*; Imperial College Press, London, **1999**.
[2] S. Trofimenko, *Chem. Rev.* **1993**, *93*, 943 – 980.
[3] S. Bieller, M. Bolte, H.-W. Lerner, M. Wagner, *Inorg. Chem.* **2005**, *44*, 9489 – 9496.
[4] S. Bieller, F. Zhang, M. Bolte, J. W. Bats, H.-W. Lerner, M. Wagner, *Organometallics* **2004**, *23*, 2107 – 2113.
[5] Zhang, M. Bolte, H.-W. Lerner, M. Wagner, *Organometallics* **2004**, *23*, 5075 – 5080.
[6] F. Zhang, T. Morawitz, S. Bieller, M. Bolte, H.-W. Lerner, M. Wagner, *Dalton Trans.* **2007**, 4594 – 4598.
[7] T. Morawitz, M. Bolte, H.-W. Lerner, M. Wagner, *Z. Anorg. Allg. Chem.* **2008**, *634*, 1409 – 1414.
[8] T. Morawitz, M. Bolte, H.-W. Lerner, M. Wagner, *Z. Anorg. Allg. Chem.* **2008**, *634*, 1570 – 1574.
[9] R. D. Adams, F. A. Cotton (Eds.): *Catalysis by Di- and Polynuclear Metal Cluster Complexes*; Wiley: New York (1988).
[10] S. Bieller, A. Haghiri, M. Bolte, J. W. Bats, M. Wagner, H.-W. Lerner, *Inorg. Chim. Acta* **2006**, *359*, 1559 – 1572.
[11] T. Morawitz, F. Zhang, M. Bolte, J. W. Bats, H.-W. Lerner, M. Wagner, *Organometallics* **2008**, *27*, 5067 – 5074.
[12] O. Graziani, L. Toupet, J.-R. Hamon, M. Tilset, *Inorg. Chim. Acta* **2002**, *341*, 127 – 131.
[13] M. Pejic, S. Popp, H.-W. Lerner, M. Wagner. Ger. Patent DE 102013012685.1, **2013**.
[14] J. Heilmann-Brohl, F. Schödel, M. Bolte, M. Wagner, H.-W. Lerner, *Z. Naturforsch.* **2011**, *66b*, 1151 – 1160.
[15] Q. Liu, M. S. Mudadu, H. Schmider, R. Thummel, Y. Tao, S. Wang, *Organometallics* **2002**, *21*, 4743 – 4749.
[16] J. M. Bentzien, H. Takahashi. Patent WO 2007/058832 A2, **2007**.
[17] J. Bentley, M. Biagetti, T. Genski, S. R. Kopf, C. P. Leslie, S. Melotto, M. Mauro. Patent WO 2008/092891 A1, **2008**.
[18] E. M. Zueva, M. M. Petrova, R. Herchel, Z. Trávníček, R. G. Raptis, L. Mathivathanan, J. E. McGrady, *Dalton Trans.* **2009**, 5924 – 5932.
[19] A. L. Rheingold, L. M. Liable-Sands, C. L. Incarvito, S. Trofimenko, *J. Chem. Soc., Dalton Trans.* **2002**, 2297 – 2301.
[20] M. I. Rodríguez-Franco, I. Dorronsoro, A. I. Hernández-Higueras, G. Antequera, *Tetrahedron Lett.* **2001**, *42*, 863 – 865.
[21] E. Font-Sanchis, F. J. Céspedes-Guirao, Á. Sastre-Santos, F. Fernández-Lázaro, *J. Org. Chem.* **2007**, *72*, 3589 – 3591.
[22] J. Zhou, P. Liu, Q. Lin, B. W. Metcalf, D. Meloni, Y. Pan, M. Xia, M. Li, T.-Y. Yue, J. D. Rodgers, H. Wang. Patent WO 2010/083283 A2, **2010**.
[23] M. Mogi, T. Kawanami, K. Yamada, K. Yasoshima, H. Imase, T. Miyake, O. Ohmori, Patent WO 2009/071509 A1, **2009**.
[24] L. Birkofer, M. Franz, *Chem. Ber.* **1972**, *105*, 1759 – 1767.
[25] A. L. Spek, *J. Appl. Crystallogr.* **2003**, *36*, 7 – 13.
[26] X-AREA, Diffractometer Control Program System, Stoe & Cie GmbH, Darmstadt (Germany) **2002**.
[27] G. M. Sheldrick, *Acta Crystallogr.* **2008**, *A64*, 112 – 122.